ISSN 1672-9145 **Acta Biochimica et Biophysica Sinica** 2006, **38**(1): 29–36 **CN** 31-1940/Q

Transforming Growth Factor-β1 Induces Transdifferentiation of Fibroblasts into Myofibroblasts in Hypoxic Pulmonary Vascular Remodeling

Yong-Liang JIANG, Ai-Guo DAI*, Qi-Fang LI, and Rui-Cheng HU

Department of Respiratory Medicine, Hunan Institute of Gerontology, Hunan Province Geriatric Hospital, Changsha 410001, China

Abstract The muscularization of non-muscular pulmonary arterioles is an important pathological feature of hypoxic pulmonary vascular remodeling. However, the origin of the cells involved in this process is still not well understood. The present study was undertaken to test the hypothesis that transforming growth factor-β1 (TGF-β1) can induce transdifferentiation of fibroblasts into myofibroblasts, which might play a key role in the muscularization of non-muscular pulmonary arterioles. It was found that mean pulmonary arterial pressure increased significantly after 7 d of hypoxia. Pulmonary artery remodeling index and right ventricular hypertrophy became evident after 14 d of hypoxia. The distribution of nonmuscular, partially muscular, and muscular vessels was significantly different after 7 d of hypoxia. Immunocytochemistry results demonstrated that the expression of α-smooth muscle actin was increased in intra-acinar pulmonary arteries with increasing hypoxic time. TGF-β1 mRNA expression in pulmonary arterial walls was increased significantly after 14 d of hypoxia, but showed no obvious changes after 3 or 7 d of hypoxia. In pulmonary tunica adventitia and tunica media, TGF-β1 protein staining was poorly positive in control rats, but was markedly enhanced after 3 d of hypoxia, reaching its peak after 7 d of hypoxia. The myofibroblast phenotype was confirmed by electron microscopy, which revealed microfilaments and a well-developed rough endoplasmic reticulum. Taken together, our results suggested that TGF-β1 induces transdifferentiation of fibroblasts into myofibroblasts, which is important in hypoxic pulmonary vascular remodeling.

Key words transforming growth factor-β1; fibroblast; myofibroblast; hypertension; lung

Chronic obstructive pulmonary disease in humans is associated with chronic hypoxia. The principal medical consequences of chronic hypoxia include polycythemia and pulmonary hypertension, and finally, cor pulmonale. Laboratory animals subjected to decreased ambient oxygen concentrations manifest similar physiological responses, resulting in the occurrence of hypoxic pulmonary hypertension. The pathophysiology of hypoxic pulmonary hypertension is complex and involves vasoconstriction as well as neomuscularisation and thickening of the media and adventitia of pulmonary arterioles. The fibroblast is the most abundant cell type in normal connective tissues and plays a central role in synthesis, degradation, and remodeling of the extracellular matrix in health and disease. The majority of fibroblasts demonstrate the ability of converting into α-smooth muscle actin (α-SMA)-containing myofibroblasts in response to specific stimuli. Myofibroblasts are "hyperactivated" fibroblasts with properties of fibroblasts and muscle cells [1–3] that facilitate tissue remodeling and wound healing and also play a pathological role in fibrotic disease. Compared with their precursor cell type (referred to as stellate transformed [4] or protomyofibroblasts [1]), activated myofibroblasts have dramatically higher levels of extracellular matrix (ECM) and cytokine secretion, increased contraction [3], and a trademark stellate morphology with prominent stress fibers. Histochemically, myofibroblasts are characterized by the expression of α-SMA. They can also express other contractile proteins, such as the striated-muscle isoforms of

Received: July 19, 2005 Accepted: September 5, 2005

This work was supported by the grants from the Foundation of Hunan Province Health Committee (No. Y02-081 and No. B2004-137) and the Foundation of Hunan Province Educational Committee (No. 03C397)

*Corresponding author: Tel, 86-731-4762793; Fax, 86-731-4735215; E-mail, daiaiguo2003@163.com

DOI: 10.1111/j.1745-7270.2006.00123.x

myosin heavy chain. Myofibroblast activation is strictly regulated by cytokines that control differentiation, proliferation, contraction, ECM secretion, and migration to the site of wound healing or tissue remodeling [3]. After completion of remodeling activities, myofibroblasts are eliminated by apoptosis; however, when the myofibroblast life cycle is not regulated properly, myofibroblasts persist with continued force generation and ECM production, resulting in pathological fibrosis, scarring, and fibrocontractile disease [5].

Transforming growth factor-β1 (TGF-β1) is involved in tissue repair by modulating the growth of mesenchymal cells, augmenting the synthesis of several ECM proteins, and facilitating the differentiation of fibroblasts [6]. Increased expression of TGF-β1 has been demonstrated in human restenotic lesions. In experimental settings systemic administration of TGF-β1 resulted in the formation of a neointima rich in ECM proteins [7]. Conversely, anti-TGF-β1 neutralizing antibodies reduced ECM proteins, further pointing to the important role of TGF-β1 in vascular repair [8]. However, the roles of TGF-β1 and myofibroblasts in the development of hypoxia-induced pulmonary hypertension and the accompanying vascular remodeling are incompletely understood. In this study, we investigate the dynamic expression of TGF-β1 and myofibroblast formation in a rat model of hypoxia.

Materials and Methods

Animals and hypoxia model

The protocol for exposure of rats to hypoxia and normoxia was identical to that reported previously by our laboratory [9]. In the present study, we used 40 male Wistar rats purchased from the Animal Experimental Center of Central South University, Changsha, China. The animals weighed 220±10 g and the average age was 6–8 weeks. They were randomly divided into five groups (eight rats in each group). Each group of hypoxic rats was exposed for a specified time period (3, 7, 14, or 21 d) for 8 h per day intermittently to normobaric hypoxia (10.0%±0.5% oxygen) in a ventilated chamber. Age- and weight-matched control rats were maintained in normobaric 21% oxygen (fresh air). To establish the hypoxic conditions the chamber was flushed with a mixture of room air and nitrogen from a liquid nitrogen reservoir. An oxygen analyser (HT-6101; Kanda Electrical, Chengdu, China) was used to monitor the chamber environment. Carbon dioxide was removed with soda lime, excess humidity removed by anhydrous calcium chloride, and boric acid was used to keep ammonia levels within the chamber to a minimum. The normoxic control rats were not kept in the chamber but they were housed in the same room and treated in the same fashion as the hypoxic rats.

Mean pulmonary arterial pressure (*mPAP*) measurement

mPAP was measured as described previously [10]. After rats were anesthetized with pentobarbital sodium (40 mg/kg intraperitoneally), a specially designed single-lumen catheter was inserted into the main pulmonary artery through the right jugular vein, at which point the position of the catheter was judged by the waveform of the pressure signal. The *mPAP* was measured with PowerLab monitoring equipment (AD Instruments, Milford, USA).

Right ventricular hypertrophy index (*RVHI*)

After the measurement of *mPAP*, the rats were killed and their lungs were collected for morphometry analysis, *in situ* hybridization and immunohistochemical examination; their hearts were collected for measurement of *RVHI*. For right ventricular hypertrophy measurement, hearts were excised and atria were removed. The right ventricular free wall was dissected, and each chamber weighed. The ratio of right ventricular weight (*RV*) to weight of left ventricle (*LV*) plus septum (*S*) [*RV*/(*LV*+*S*)] was used as an index of right ventricular hypertrophy.

Vessel morphometric analysis and constituent ratio of the three types of pulmonary vessels in the intra-acinus pulmonary artery

Four micrometer lung sections were embedded in paraffin, stained with hematoxylin-eosin, then examined using light microscopy. At least five representative pulmonary arterioles (outer diameter approximately 100–150 μm), chosen from three different sections from each animal, were independently examined. The images of the arterioles were captured and analysed with PIPS-2020 Image software (Chongqing Tianhai Company, Chongqing, China). To evaluate hypoxic pulmonary vascular remodeling, the ratio of vascular wall area to external diameter (*WA*%), the ratio of vascular lumen area to total area (*LA*%), the number of smooth muscle cell nuclei in pulmonary arteriole tunica media (*SMC*; per 1000 μm^2) and pulmonary artery media thickness were obtained. The total number of intra-acinus pulmonary artery of unit area (25 mm^2) was counted. Moreover, the constituent ratio of nonmuscular, partially muscular, and muscular arteries was obtained.

In situ hybridization of TGF-β1

In situ hybridization was performed using a detection kit (Wuhan Boster Biological Technology, Wuhan, China). The oligonucleotide probes (Wuhan Boster Biological Technology) were designed according to the TGF-β1 sequences of rat. The sequences of probes against TGF-β1 mRNA were: 5′-ACCTGCAAGACCATCGACATGGAGCTGGTG-3′; 5′-TGTACAACAGCACCCGCGACCGGGTGGCAG-3′; 5′-CTACCAGAAATATAGCAACAATTCCTGGCG-3′.

Hybridization was performed on serial sections of formalin-fixed (containing 0.1% diethylpyrocarbonate) paraffin-embedded lung tissues according to manufacturer's instructions. Briefly, sections were digested with pepsin for 20 min at 37 ºC. After 2 h of prehybridization, sections were incubated with digoxin-labeled single-stranded oligonucleotide probes for 16 h at 38 ºC (negative controls were incubated with blank probe solution). After unbound probes were washed off, sections were incubated with rabbit antibodies against digoxin and with biotinylated goat-antirabbit secondary antibodies. Afterwards, sections were incubated with streptavidin-horseradish peroxidase (HRP) and visualized by a color reaction with diaminobenzidine (Wuhan Boster Biological Technology). Brown and yellow colours indicated positive results. Finally, the sections were counterstained with hematoxylin and mounted. Expression levels of mRNA were quantified by a pathology image analysis system (PIPS-2020).

Immunohistochemistry analysis of TGF-β1 and α-SMA

A streptavidin-biotin complex kit (Wuhan Boster Biological Technology) was used for immunohistochemisty, which was performed similar to that described previously with minor modifications. Briefly, serial sections of formalin-fixed paraffin-embedded lung tissues were digested with 3% H_2O_2 for 20 min at room temperature, then preincubated with 10% non-immunized serum. Sections were incubated with rabbit anti-TGF-β1 or anti-α-SMA polyclonal antibody (at a working dilution of 1:100) overnight at 4 ºC (negative controls were incubated with phosphate-buffered saline only). After unbound antibodies were washed off, the sections were incubated with biotinylated goat-antirabbit secondary antibodies and thereafter incubated with streptavidin-HRP. Subsequently, sections were visualized by a color reaction with diaminobenzidine as the substrate. Brown and yellow colours indicated positive results (mainly cytoplasm). Finally, the sections were counterstained with hematoxylin (resulting in blue nuclei) and mounted. Expression levels of protein were quantified by a pathology image analysis system (PIPS-2020).

Electron microscopy

For electron microscopy, tissue cultures were fixed in cold 2.5% glutaraldehyde in 0.1 M of sodium cacodylate buffer and postfixed in a solution of 1% osmium tetroxide, dehydrated, and embedded in a standard fashion. The specimens were then embedded, sectioned, and stained by routine means for a JEO-1200 electron microscope (JEOL, Tokyo, Japan).

Statistical analysis

Data were expressed as mean±SD. The group *t*-test was used to compare data between two groups. ANOVA was used to determine statistically significant differences among multiple groups, with the Newman-Keuls test comparing statistical significance between two groups. Categorical data were expressed as frequency distribution and the χ^2 test was used. $P<0.05$ was considered as statistically significant.

Results

Chronic hypoxia increased *mPAP*

mPAP was measured as an indicator of pulmonary artery pressure in conscious rats. *mPAP* in normoxic rats was 14.02±0.41 mmHg. As expected, the hypoxic animals developed pulmonary hypertension after 7 d of exposure to hypoxia ($P<0.05$), reaching its peak level after 14 d of hypoxia, then remained on the high level (**Table 1**).

Chronic hypoxia leads to hypoxic pulmonary vascular remodeling and right ventricular hypertrophy

As shown in **Table 1**, pulmonary arterioles in normoxic animals were thin, whereas after 7 d of hypoxic exposure, they developed increased medial thickness characteristic of pulmonary hypertension. Quantification of these structural changes in several lung sections of all of the animals exposed to each of the different hypoxia time periods (3, 7, 14 or 21 d) revealed significantly increased medial thickness of pulmonary arterioles in hypoxic animals in comparison with normoxic controls. Right ventricular hypertrophy resulting from right ventricle pressure overload is a hallmark of pulmonary hypertension. After 14 d of hypoxia, *RVHI* was significantly increased in comparison with the control ($P<0.05$). *RVHI* had increased further after 21 d of hypoxia. This result indicated right ventricu-

Table 1 Effects of different time periods of hypoxia on *mPAP*, right ventricular hypertrophy, and pulmonary artery remodeling in rats

Group	*mPAP* (mmHg)	*LA* (%)	*WA* (%)	*SMC*	*PAMT* (μm)	*RV*/(*LV*+*S*) (%)
Control	14.02±0.41	64.5±1.3	35.5±1.3	5.5±1.0	11.9±0.6	23.6±0.5
Hypoxia for 3 d	14.58±0.28	63.0±0.9	37.0±0.8	5.8±0.8	12.0±0.5	23.3±1.7
Hypoxia for 7 d	18.41±0.37[ac]	52.2±0.8[ac]	47.8±0.8[ac]	6.1±0.8	12.3±0.5	24.0±0.9
Hypoxia for 14 d	21.17±0.23[acd]	39.7±0.4[acd]	60.3±0.4[acd]	7.1±0.8[acd]	15.0±0.3[acd]	25.0±1.8[ac]
Hypoxia for 21 d	22.24±0.21[bcd]	35.0±0.7[bcde]	65.0±0.7[acde]	9.1±0.8[acde]	23.0±0.8[acde]	27.7±1.0[bcd]

[a] $P<0.05$ compared with the control group; [b] $P<0.01$ compared with the control group; [c] $P<0.05$ compared with hypoxia for 3 d; [d] $P<0.05$ compared with hypoxia for 7 d; [e] $P<0.05$ compared with hypoxia for 14 d. *mPAP*, mean pulmonary arterial pressure; *LA*, the ratio of vascular lumen area to total area; *PAMT*, pulmonary artery media thickness; *RV*/(*LV*+*S*), the ratio of right ventricular weight to weight of left ventricle plus septum; *SMC*, the number of smooth muscle cell nuclei in pulmonary arteriole media per 1000 μm^2; *WA*, the ratio of vascular wall area to external diameter. Data are represented as mean±SD (n=8).

lar hypertrophy had developed after 14 d of exposure to hypoxia.

Changes of constituent ratios of three types of pulmonary arterioles after hypoxia

We observed the distribution of arterioles by wall structure in hypoxia-induced pulmonary hypertension. The distribution of nonmuscular, partially muscular, and muscular arterioles was significantly different ($P<0.05$) from 7 d in alveolar wall arterioles; muscular and partially muscular arteries increased at the expense of nonmuscular arterioles (**Fig. 1**).

Dynamic analysis of α-SMA in alveolar wall arterioles

In both normal and hypoxic lungs, bronchial smooth muscle cells and the smooth muscle cells of pre-acinar vessels associated with bronchioli and terminal bronchioli expressed α-SMA. In the normal lung, in the thick-walled oblique muscular artery, and in arterioles associated with respiratory bronchioli at the entrance to the acinus, cells expressing α-SMA were evident [**Table 2** and **Fig. 2(A)**]. Alveolar duct and alveolar wall arterioles with cells expressing α-SMA were rare. Initially in hypoxia (3 d), the distribution of α-SMA cells was similar to that throughout the normal lung [**Table 2** and **Fig. 2(B)**]. By 7 d, increased numbers of α-SMA cells were evident in pre-acinar arterioles of the hypoxic lung, but most intra-acinar arterioles were still negative. At 14 d, alveolar arterioles with α-SMA cells increased and septal cells at the entrance to alveolar ducts were also positive [**Table 2** and **Fig. 2(C)**]. By 21 d, the number and intensity of α-SMA cells had increased and small thick-walled alveolar wall and duct arterioles with these cells were evident, including arterioles with muscular walls as well as partially muscular

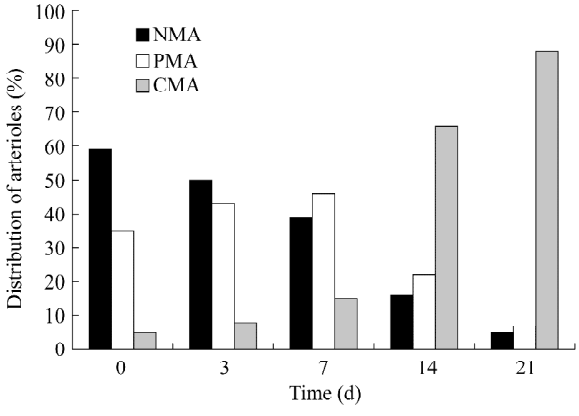

Fig. 1 Changes of composition of nonmuscular arteriole (NMA), partially muscular arteriole (PMA) and muscular arteriole (CMA) in rat after different time periods of hypoxia

Table 2 Comparison of α-smooth muscle actin (α-SMA) expression in the wall of pulmonary arterioles of rat after different time periods of hypoxia

Group	α-SMA
Control	0.1052±0.0084
Hypoxia for 3 d	0.1123±0.0092
Hypoxia for 7 d	0.1228±0.0098[ab]
Hypoxia for 14 d	0.1345±0.0104[acd]
Hypoxia for 21 d	0.1428±0.0110[ace]

[a] $P<0.01$ compared with the control group; [b] $P<0.05$ compared with hypoxia for 3 d; [c] $P<0.01$ compared with hypoxia for 3 d; [d] $P<0.05$ compared with hypoxia for 7 d; [e] $P<0.01$ compared with hypoxia for 7 d. Optical density values are represented as mean±SD (n=10).

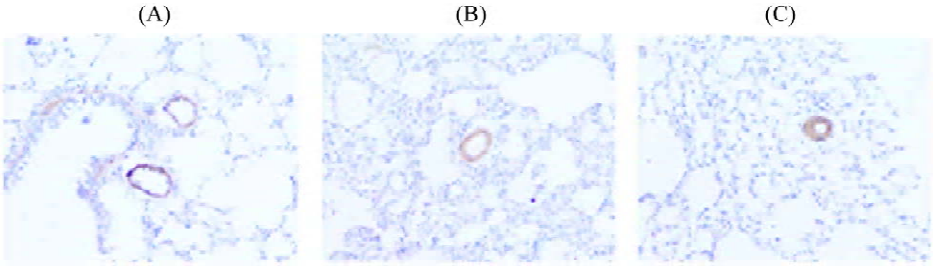

Fig. 2 Immunohistochemistry analysis of α-smooth muscle actin (α-SMA) protein expression in smooth muscle of pulmonary arteries in rat

(A) α-SMA expression in smooth muscle of pulmonary vessels and bronchi in the control group. Magnification, 200×. (B) α-SMA expression in intra-acinar pulmonary arteries 3 d after hypoxia. Magnification, 200×. (C) α-SMA expression in intra-acinar pulmonary arteries 14 d after hypoxia. Magnification, 200×.

arterioles. All of the distal thick-walled arterioles had α-SMA cells.

Hypoxia induces TGF-β1 mRNA and protein expression in pulmonary arterial walls

Table 3 shows control pulmonary arterioles displayed low-level expression of TGF-β1 transcripts in medial *SMCs*. Adventitial fibroblasts also showed a paucity of TGF-β1 transcripts, TGF-β1 mRNA expression in pulmonary arterial walls was increased significantly after 14 and 21 d of hypoxia, but showed no obvious changes after 3 or 7 d of hypoxia [**Fig. 3(A–C)**]. TGF-β1 mRNA was located predominantly in tunica adventitia and tunica media. In pulmonary arterioles tunica adventitia and tunica media, TGF-β1 protein staining was poorly positive in control rats, but was markedly enhanced after 3 and 7 d of hypoxia, then weakened after 14 and 21 d of hypoxia [**Fig. 4(A–C)**].

Table 3 Effects of different time periods of hypoxia on expression of transforming growth factor (TGF)-β1 gene in pulmonary arteries of rats

Group	TGF-β1 protein	TGF-β1 mRNA
Control	0.042±0.012	0.145±0.018
Hypoxia for 3 d	0.198±0.031[a]	0.163±0.021
Hypoxia for 7 d	0.267±0.035[ab]	0.176±0.026
Hypoxia for 14 d	0.143±0.026[abc]	0.385±0.028[abc]
Hypoxia for 21 d	0.125±0.015[abc]	0.413±0.025[abc]

[a] $P<0.01$ compared with control group; [b] $P<0.01$ compared with hypoxia for 3 d; [c] $P<0.01$ compared with hypoxia for 7 d. Data are represented as mean±SD (n=8).

Ultrastructural characteristics of adventitial myofibroblast and analysis of cell phenotype in alveolar wall arterioles

To examine the ultrastructural changes associated with TGF-β1 induction, the smallest vessels were examined by

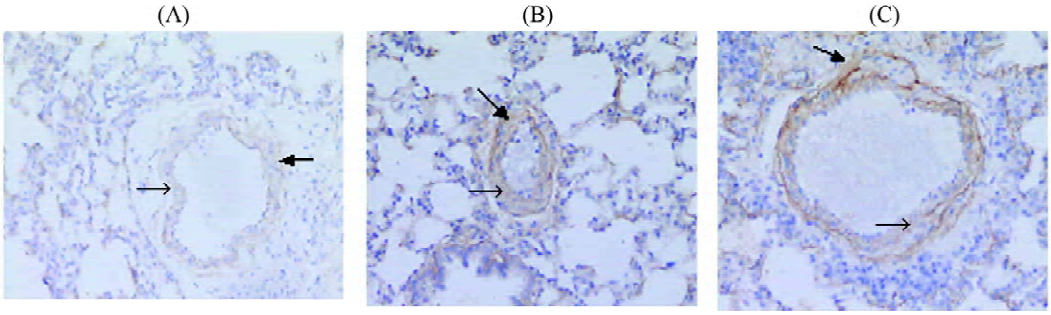

Fig. 3 *In situ* hybridization of transforming growth factor (TGF)-β1 mRNA expression in pulmonary arteries of rat

(A) Pulmonary artery of control. In arterial adentitia (black arrow) and media (blank arrow), TGF-β1 mRNA staining was poorly positive. Magnification, 200×. (B) Pulmonary artery after hypoxia for 7 d. In arterial adentitia (black arrow) and media (blank arrow), TGF-β1 mRNA staining was poorly positive. Magnification, 200×. (C) Pulmonary artery after hypoxia for 14 d. In arterial adentitia (black arrow) and media (blank arrow), TGF-β1 mRNA staining was strongly positive. Magnification, 200×.

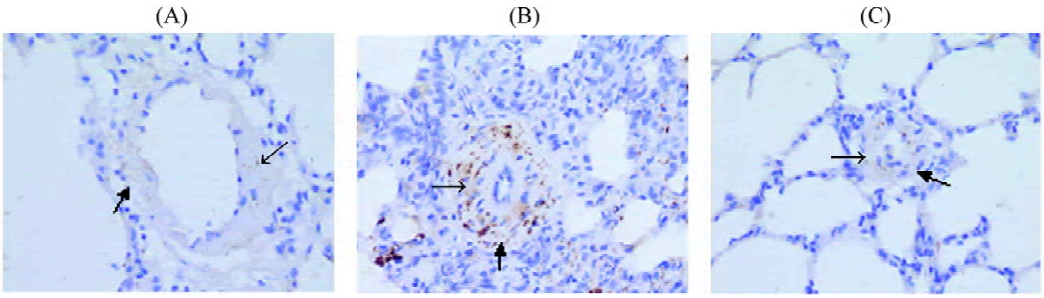

Fig. 4 Immunohistochemistry analysis of transforming growth factor (TGF)-β1 protein expression in pulmonary arteries of rat
(A) Pulmonary artery of control. In arterial adentitia (black arrow) and media (blank arrow), TGF-β1 protein staining was poorly positive. Magnification, 200×. (B) Pulmonary artery after hypoxia for 7 d. In arterial adentitia (black arrow) and media (blank arrow), TGF-β1 protein staining was strongly positive. Magnification, 200×. (C) Pulmonary artery after hypoxia for 14 d. In arterial adentitia (black arrow) and media (blank arrow), TGF-β1 protein staining was poorly positive. Magnification, 200×.

electron microscopy. In the normal lung, they were constituted in alveolus and endothelial cells [**Fig. 5(A)**], but at the late stage of hypoxia (21 d), myofibroblast phenotype was organized between elastic laminae. Aligning fibroblasts were associated with the wall. Myofibroblasts formed the walls of the smallest vessels [**Fig. 5(B)**]. All of these cells were well-developed microfilaments.

Discussion

Hypoxic pulmonary vascular remodeling is an important pathological feature of hypoxic pulmonary hypertension, leading to increased pulmonary vascular resistance and reduced compliance. It involves thickening of all three layers of the blood vessel wall (due to hypertrophy and/or hyperplasia of the predominant cell type within each layer), as well as extracellular matrix deposition. Neomuscularisation of non-muscular arteries and neo-intimal lesions also occur [11]. But the cell origin is unclear for the muscularization of non-muscular pulmonary arterioles in hypoxic pulmonary vascular remodeling. Our results demonstrate that the hypoxic animals developed pulmonary hypertension after 7 d of exposure to hypoxia; after 14 and 21 d, hypoxic animals showed significantly increased medial thickness of pulmonary arterioles and the muscularization of non-muscular pulmonary arterioles compared with normoxic controls.

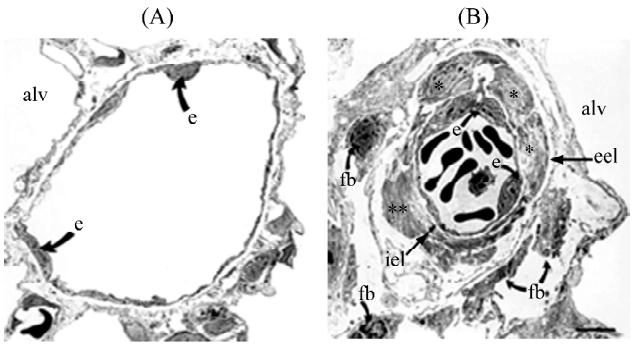

Fig. 5 Ultrastructural characteristics of alveolar wall arteries in rat associated with transforming growth factor-β1 induction
(A) Ultrastructural characteristics of alveolar wall vessels in control lung. Small, thin-walled alveolar wall vessel with the alveolus (alv) and endothelia cells (e) Magnification, 5000×. (B) Ultrastructural characteristics of alveolar wall vessels after hypoxia for 21 d. Myofibroblasts (asterisks) are organized between elastic laminae (iel, internal elastic lamina; eel, external elastic lamina). Aligning fibroblasts are associated with the wall (fb). Magnification, 5000×.

Myofibroblasts represent highly specialized mesenchymal cells that play a central role in tissue repair. However, very little is known about the important role myofibroblast differentiation might play in hypoxic pulmonary vascular remodeling. We designed our experiments to specifically characterize the myofibroblast phenotype, its induction by TGF-β1, and the potential contribution to pathological changes in hypoxic pulmonary vascular remodeling. Here, we demonstrate that myofibroblast formation contributes to muscularization of non-muscular pulmonary arterioles and TGF-1 is capable of inducing myofibroblast differentiation. Their formation is marked by the development of bundles of microfilaments (stress fibers) and abundant connections with the surrounding ECM. One of the most prominent features of TGF-β1-inducing fibroblasts is the appearance of α-SMA-positive myofibroblasts. Our results demonstrate that in hypoxic pulmonary vascular remodeling, the predominant contribution to myofibroblast

generation comes from resident fibroblasts, and others have identified TGF-β1 as the key molecular switch in myofibroblast generation [12,13]. Moreover, hypoxia might also induce differentiation of pulmonary artery adventitial fibroblasts into myofibroblasts [14]. These characteristics are consistent with the primary role of newly-formed myofibroblasts to close an open wound by means of ECM protein synthesis (e.g., collagens) and contraction. Subsequent studies have confirmed the presence of myofibroblasts in a wide range of other pathological conditions that are associated with fibrogenesis and organ remodeling [15,16].

TGF-β1 is a member of the TGF-β cytokine superfamily that coordinates differentiation of mesenchymal stem cells during such distinct processes as organogenesis, bone and neuronal tissue formation, and myofibroblast activation [17]. In the present study, hypoxia induced dynamic changes in TGF-β1 expression, with the initial changes involving the adventitia and media, as reflected by *in situ* hybridization and immunohistochemistry findings. The increase in TGF-β1 mRNA in adventitial and medial cells was apparent as early as 3 d after hypoxia. The question can be raised as to the mechanism(s) of TGF-β1 induction after vascular hypoxia, inasmuch as normal adventitial fibroblasts are devoid of this cytokine. The ability of TGF-β1 to induce its own expression suggests that its release from degranulated platelets and activated macrophages might initiate TGF-β1 upregulation in adventitial fibroblasts [18]. Furthermore, platelet-derived growth factor released from platelets early after vascular insult could contribute to the induction of TGF-β1 [19]. Interestingly, the TGF-β1 mRNA was not significantly increased until 14 d of hypoxia, yet TGF-β1 protein was markedly increased after only 3 d of hypoxia. Moreover, after 14 and 21 d of hypoxia, when the TGF-β1 mRNA levels were at their highest, protein levels started to drop. This suggests a major alteration in post-transcriptional regulation.

In vivo and *in vitro* studies indicate that TGF-β1 is one of the main inducers of the differentiation of fibroblasts into myofibroblasts [12,13]. Prior studies have shown that TGF-β1 induces adventitial myofibroblast differentiation using a protein kinase Cα-dependent process [20]. The origin of myofibroblasts in various tissues has been a subject of controversy [21]. The augmented synthetic function of myofibroblasts derived from various tissues, with the accompanying deposition of collagens and fibronectin, is consistent with the profibrotic effects of TGF-β1 [22]. Furthermore, myofibroblasts are capable of mediating contraction of their surrounding environment.

Hypoxia might initiate a series of cellular events leading to hypoxic pulmonary vascular remodeling. Intervention at this stage of the disease might prevent the development of structural changes and the progression to hypoxic pulmonary vascular remodeling. Through elucidation of the pathologic importance of TGF-β1 in fibroblast-differentiated myofibroblasts, we expect the availability of specific TGF-β1 antagonists. The present study provides new information about myofibroblast formation and its contribution to the muscularization of non-muscular pulmonary arterioles. Further elucidation of the origin of myofibroblasts might reveal clues for approaches to curing hypoxic pulmonary hypertension.

References

1 Tomasek JJ, Gabbiani G, Hinz B, Chaponnier C, Brown RA. Myofibroblasts and mechano-regulation of connective tissue remodelling. Nat Rev Mol Cell Biol 2002, 3: 349–363

2 Walker GA, Guerrero IA, Leinwand LA. Myofibroblasts: Molecular crossdressers. Curr Top Dev Biol 2001, 51: 91–107

3 Powell DW, Mifflin RC, Valentich JD, Crowe SE, Saada JI, West AB. Myofibroblasts. I. Paracrine cells important in health and disease. Am J Physiol Cell Physiol 1999, 277: 1–19

4 Serini G, Gabbiani G. Mechanisms of myofibroblast activity and phenotypic modulation. Exp Cell Res 1999, 250: 273–283

5 Rice NA, Leinwand LA. Skeletal myosin heavy chain function in cultured lung myofibroblasts. J Cell Biol 2003, 163: 119–129

6 Jarmuz T, Roser S, Rivera H, Gal A, Roman J. Transforming growth factor-beta1, myofibroblasts, and tissue remodeling in the pathogenesis of tracheal injury: Potential role of gastroesophageal reflux. Ann Otol Rhinol Laryngol 2004, 113: 488–497

7 Lijnen P, Petrov V. Transforming growth factor-beta 1-induced collagen production in cultures of cardiac fibroblasts is the result of the appearance of myofibroblasts. Methods Find Exp Clin Pharmacol 2002, 24: 333–344

8 Burgess HA, Daugherty LE, Thatcher TH, Lakatos HF, Ray DM, Redonnet M, Phipps RP *et al*. PPARγ agonists inhibit TGF-β induced pulmonary myofibroblast differentiation and collagen production: Implications for therapy of lung fibrosis. Am J Physiol Lung Cell Mol Physiol 2005, 288: 1146–1153

9 Hu RC, Dai AG, Tan SX. Hypoxia-inducible factor 1 alpha upregulates the expression of inducible nitric oxide synthase gene in pulmonary arteries of hypoxic rat. Chin Med J 2002, 115: 1833–1837

10 Li QF, Dai AG. Hypoxia inducible factor-1 alpha correlates the expression of heme oxygenase 1 gene in pulmonary arteries of rat with hypoxia-induced pulmonary hypertension. Acta Biochim Biophys Sin 2004, 36: 133–140

11 Jeffery TK, Wanstall JC. Pulmonary vascular remodeling: A target for therapeutic intervention in pulmonary hypertension. Pharmacol Ther 2001, 92: 1–20

12 Thannickal VJ, Lee DY, White ES, Cui Z, Larios JM, Chacon R, Horowitz JC *et al*. Myofibroblast differentiation by transforming growth factor-β1 is dependent on cell adhesion and integrin signaling via focal adhesion kinase. J Biol Chem 2003, 278: 12384–12389

13 Arora PD, McCulloch CA. The deletion of transforming growth factor-β-induced myofibroblasts depends on growth conditions and actin organization. Am J Pathol 1999, 155: 2087–2099

14 Short M, Nemenoff RA, Zawada WM, Stenmark KR, Das M. Hypoxia induces differentiation of pulmonary artery adventitial fibroblasts into myofibroblasts. Am J Physiol Cell Physiol 2004, 286: 416–425
15 Reisdorf P, Lawrence DA, Sivan V, Klising E, Martin MT. Alteration of transforming growth factor-β1 response involves down-regulation of Smad3 signaling in myofibroblasts from skin fibrosis. Am J Pathol 2001, 159: 263–272
16 Desmouliere A, Chaponnier C, Gabbiani G. Tissue repair, contraction, and the myofibroblast. Wound Repair Regen 2005, 13: 7–12
17 Piek E, Heldin CH, Ten Dijke P. Specificity, diversity, and regulation in TGF-β superfamily signaling. FASEB J 1999, 13: 2105–2124
18 Huynh ML, Fadok VA, Henson PM. Transforming growth factor-β_1 secretion from murine macrophages is released by *in vivo* ingestion of apoptotic cells. Chest 2001, 120: 3
19 Fraser D, Wakefield L, Phillips A. Independent regulation of transforming growth factor-β1 transcription and translation by glucose and platelet-derived growth factor. Am J Pathol 2002, 161: 1039–1049
20 Gao PJ, Li Y, Sun AJ, Liu JJ, Ji KD, Zhang YZ, Sun WL *et al*. Differentiation of vascular myofibroblasts induced by transforming growth factor-beta1 requires the involvement of protein kinase Calpha. J Mol Cell Cardiol 2003, 35: 1105–1112
21 Petrov VV, Fagard RH, Lijnen PJ. Transforming growth factor-beta (1) induces angiotensin-converting enzyme synthesis in rat cardiac fibroblasts during their differentiation to myofibroblasts. J Renin Angiotensin Aldosterone Syst 2000, 1: 342–352
22 Malmström J, Lindberg H, Lindberg C, Bratt C, Wieslander E, Delander EL, Särnstrand B *et al*. Transforming growth factor-β_1 specifically induce proteins involved in the myofibroblast contractile apparatus. Mol Cell Proteomics 2004, 3: 466–477

Edited by
Ming-Hua XU